Circatidal control of gene expression in the deep-sea hot vent shrimp *Shinkaicaris leurokolos*

Hongyin Zhang[1,2¶], Takuya Yahagi[3¶], Norio Miyamoto[4], Chong Chen[4], Qingqiu Jiang[1,2], Pei-Yuan Qian[5,6], and Jin Sun[1,2*]

1 Key Laboratory of Evolution & Marine Biodiversity (Ministry of Education) and Institute of Evolution & Marine Biodiversity, Ocean University of China, Qingdao 266003, China

2 Laoshan Laboratory, Qingdao 266237, China

3 Department of Marine Ecosystems Science, Atmosphere and Ocean Research Institute, The University of Tokyo, 5-1-5 Kashiwanoha, Kashiwa, Chiba 277-8564, Japan

4 X-STAR, Japan Agency for Marine-Earth Science and Technology (JAMSTEC), 2-15 Natsushima-cho, Yokosuka, Kanagawa 237-0061, Japan

5 Department of Ocean Science, Hong Kong University of Science and Technology, Clear Water Bay Road, Hong Kong SAR, China

6 Southern Marine Science and Engineering Guangdong Laboratory (Guangzhou), Guangzhou, China

* Corresponding author

E-mail: jin_sun@ouc.edu.cn

¶ These authors contributed equally to this work

Abstract

Biological clocks are a ubiquitous feature of all life, enabling the use of natural environmental cycles to track time. Although studies on circadian rhythms have contributed greatly to the knowledge of chronobiology, biological rhythms in dark biospheres such as the deep sea remain poorly understood. Despite a lack of day-night cycles, the deep sea is still affected by the tide, and some recent evidences suggest that the tidal cycle likely has non-negligible temporal effects on deep-sea organisms. Here, based on a free-running experiment, we reveal potentially endogenous biological rhythms in the gene expression of the deep-sea hydrothermal vent shrimp *Shinkaicaris leurokolos*. Oscillations with ~12-hour periods, likely reflecting tidal influence, greatly prevail over others in the temporal transcriptome. The tidal oscillated rhythms exhibit an antiphased expression pattern divided into two internally synchronized clusters, correlated with wide-ranging biological processes in the nucleus and cytoplasm, respectively. In some cases, circadian clock genes are necessary for circatidal rhythms and can be adjusted to tidal frequency. However, almost none of the identified *S. leurokolos* circadian clock genes show obvious rhythmicity, likely indicating an independent circatidal clock. These findings provide new insights into the temporal adaptations in deep-sea organisms and suggest that deep-sea hydrothermal vent organisms may be intriguing models for chronobiological studies.

Introduction

As an adaptation to natural periodic environmental changes, biological clocks have been evolving in all kingdoms of life to keep track of time [1-3]. Numerous organisms anticipate daily changes including light, temperature, and food availability, resulting in persistent rhythms dominated by circadian periodicity of ~24 hours at behavioral, physiological, and molecular levels [4-6]. To achieve this, animals rely on their internal circadian clock systems like transcription-translation feedback loops (TTFLs) that can be entrained to match the environmental cycles [7]. In dark biospheres such as the underground and deep-sea habitats, however, the absence of sunlight veils organisms there from the direct effects of everlasting day-night transitions. How organisms living in the dark schedule their activities through time, as an adaptation to darkness, remains obscure [8, 9].

The deep ocean, the largest but the least studied habitat on Earth [10], is of great interest for chronobiology research due to its distinct ecological environment [11]. With increasing depth the intensity, spectral composition, and degree of polarization of sunlight decrease dramatically, and are eventually absorbed and scattered completely at approximately 1000 m [12]. From the ecological perspective, it is more appropriate for deep-sea organisms to synchronize their biological rhythms with other zeitgebers (e.g., geophysical cycles) instead of the light cycle [13, 14]. Indeed, various environmental fluctuations related to tidal cycles have been observed in the deep, especially in hydrothermal vent ecosystems [15-18]. Vent faunas rely strongly on their local environment, and survive on organic compounds produced by chemosynthetic microbes through chemosynthesis utilizing dissolved chemicals in the vent fluids [19]. Therefore, vent animals are likely to be affected by spatial and temporal variations in environmental factors modulated by tides. Several previous studies have reported potential tide-related rhythms of behavior and community dynamics in deep-sea organisms from chemosynthetic ecosystems [13, 20-22], and a recent study revealed tidal cycles dominated the gene expression of the deep-sea vent mussel *Bathymodiolus azoricus* through periodic *in situ* sampling across 24.8 hours [23]. Although these evidences suggest that vent organisms exhibit biological rhythms in the wild, whether they need endogenous rhythms or clocks to accommodate and anticipate local environmental changes to maximize their fitness is still poorly understood.

In the Iheya North hydrothermal vent field of the Okinawa Trough, the alvinocaridid shrimp *Shinkaicaris leurokolos* lives in close proximity to the vigorously venting orifice

(0.2-0.8 m and occasionally less than 0.2 m from the vent [24]) where the hot plume and cold surrounding seawater mix spontaneously and dramatically (Fig 1A and 1B) [25]. This differs from bathymodioline mussels that inhabit more peripheral areas of vent fields (0.8-2.5 m and mostly greater than 2.5 m from the vent orifice [24]). In the central areas where *S. leurokolos* occurs, however, environmental factors fluctuate frequently at the seconds-minutes scale due to the vigorous mixing between hot vent fluid and cold surrounding seawater, possibly masking any detectable tidal effects in terms of temperature and chemistry. Considering the trade-off between tolerance and escape response [26-28], perhaps an internal clock could help *S. leurokolos* respond to occasional events (e.g., temperature anomalies) [29]. Therefore, we hypothesised that *S. leurokolos* could schedule its activities either by direct response to environmental changes or by an endogenous clock. Here, we addressed the biological rhythms of gene expression in the vent shrimp *S. leurokolos* and tested if it can maintain rhythmicity under constant environmental conditions through a free-running experiment across 72 hours.

Results and discussion

Transcriptome analysis of deep-sea vent shrimp *S. leurokolos*

We reanalysed a published long-term temperature measurement (Mean ± SD = 4.4 ± 0.1□) [30] recorded at the periphery of the Iheya North vent field where bathymodioline mussels typically occur, and found a steady semidiurnal tidal cycle with a periodicity of 12.4 hours (Fig 1C). Despite that, the temperature measured in the *S. leurokolos* colony rapidly fluctuated between 7.63 to 17.74°C in approximately 2.5 minutes (Mean ± SD = 10.16 ± 1.71°C), and other environmental factors likely co-vary in the same period (Fig 1D) [31]. This dynamic environment likely masks any detectable tidal signals, which could be potential synchronization cues for *S. leurokolos*.

S. leurokolos shrimps were then collected from the top of the actively venting NBC mound at the Original Site of Iheya North hydrothermal vent field (126°53.80’E, 27°47.45’N; 982 m depth) (Fig 1B), and immediately recovered in a temperature-insulated biobox. Once on-board the ship, shrimps were transferred into a lightproof seawater container in a dark cold room set to 4°C for the subsequent free-running experiment. To our knowledge, the localization of the central clock in crustaceans remains unclear [32], we thus fixed the whole cephalothorax and abdominal segments of each shrimp every 4 hours for a total duration of 72 hours to see the overall gene expressions in *S. leurokolos*.

The reference *de novo* transcriptome assembled from 57 samples (3 replicates per time point) comprised 313,108 contigs with an N50 of 720 bases and contained 90,755 predicted open reading frames (ORFs), which showed 92% completeness (S:83.8%, D:8.2%) with the BUSCO score. Candidate protein-coding transcripts with low expression were filtered out, leaving 23,905 transcripts with a 60.4% annotation rate for rhythmic analyses. A principal components analysis (PCA) of normalized gene expression showed a rough trend from the start of sampling (0 hours) to the end (72 hours, S1A Fig). Performing the Mann-Kendall trend test on the raw dataset, we found that 10,273 transcripts (i.e., 42.97% of the transcriptome) had a significant monotonic trend (P-value < 0.05). The trend was then removed using CEEMDAN [33] to produce a steady baseline and enhance the strength of rhythm detection methods (S1B Fig) [34]. In the PCA results plotted using detrended gene expression, the trend disappeared and sample points from different sampling times clustered together (Fig 1E), indicating a minimal external effect on the experiment as the shrimps were seemingly experiencing the same conditions.

General biological rhythms in the temporal transcriptome of *S. leurokolos*

We first used the eigenvalue/pencil [35] and ECHO [36] algorithms to carry out unbiased identification of any potential periodic oscillations in the gene expression of *S. leurokolos*. The results uncovered similar rhythmicity that most cycling transcripts were identified as ultradian rhythms, which oscillated in the tidal range of 10-14 hours, while much fewer cycling transcripts oscillated in the daily range of 22-26 hours (Fig 2A). The eigenvalue/pencil algorithm was able to identify superimposed oscillations from one cycling transcript. For cycling transcripts with multiple components composed of tidal and daily oscillations, the amplitude of the tidal component is significantly larger (Fig 2B), suggesting a stronger rhythmicity. Despite the high sensitivity of detecting weak ultradian rhythms, the eigenvalue/pencil method could have high positive false rates [37]. To validate the results, we compared several statistical rhythm detection methods (S1 Table), and then detected cycling transcripts with two robust nonparametric algorithms, RAIN [38] and empirical JTK_CYCLE (eJTK) [39]. Searching for cycling transcripts (FDR < 0.05) with periods in the range of 8-28 hours at regular intervals of 4 hours, we found the number of rhythmic transcripts identified by RAIN and eJTK both reached a peak at the 12-hour period that corresponded to a tidal cycle (S2A Fig). Interestingly, the Venn diagram showed that ECHO shared many common cycling transcripts with RAIN (60.8% of transcripts) and eJTK (65.8% of

transcripts) but detected numerous extra tidal transcripts (Fig 2C), likely due to the inclusiveness of identifying different harmonics of oscillating elements [40]. Combining the results of these three methods, we identified a total of 8,122 rhythmic transcripts (33.98% of the transcriptome) in the tidal range (Fig 2C), versus 1,230 rhythmic transcripts (5.15% of the transcriptome) in the daily range (Fig 2D). We then calculated the root mean square (RMS) amplitude using LimoRhyde2 [41] to estimate the biological effect sizes and found the tidal transcripts generally exhibited stronger rhythmicity (Fig 2E).

Notably, there was an overlap of 600 rhythmic transcripts between the tidal oscillated group and the daily oscillated group (S2B Fig). Ostensibly, 24-hour daily patterns could not only reflect circadian effects but also generate in parallel with mixed semidiurnal tidal cycles (see S2C Fig), diurnal tidal cycles, and inertial oscillations (about 26.4 hours at the sampling latitude). Here, influences of the latter two can be excluded according to the Lomb-Scargle periodogram analysis performed before (see Fig 1C). Nearly 60% of the overlapped transcripts obtained lower adjusted *P*-values when identified as tidal oscillations rather than daily oscillations, reflecting higher statistical significance in the tidal component (S2D Fig). Furthermore, we calculated the RMS amplitude of tidal and daily components and the results showed that most transcripts had larger amplitude in tidal oscillations, indicating the tidal cycles contribute more biologically relevant effects to the overlapping rhythmic transcripts (S2E Fig). Therefore, in the temporal transcriptome of *S. leurokolos*, the proportion of rhythmic transcripts dominated by approximately 24-hour daily cycles is considerably less than the value obtained statistically, and the former is likely close to the proportion (2.6% of the transcriptome) reported in the previous study on deep-sea vent mussels [23].

These results demonstrate sustainable endogenous rhythmic gene expression in *S. leurokolos* under constant conditions. The temporal transcriptome is dominated by the approximately 12-hour tidal rhythms, which greatly prevail over other oscillations with different periods, especially the 24-hour daily transcripts that are likely unrelated to the circadian rhythm.

Patterns of tidal gene expression in *S. leurokolos*

To uncover the biological rhythms ticking in the deep, we then focused on the dominant tidal rhythms in the temporal transcriptome of *S. leurokolos*. Our 72-hour duration of sampling covered approximately six tidal cycles, allowing us to test the stability and

robustness of rhythmicity in the tidal gene expression [41]. To capture the amplitude changes over time, we fitted the gene expression to an extended fixed-amplitude model using ECHO [36] and categorized the results into different oscillation types based on the value of the amplitude change coefficient (see Materials and methods for details). For convenience of analysis, we concentrated on the tidal transcripts identified by the ECHO algorithm (Benjamini-Hochberg corrected *P*-values < 0.05). The analysis revealed five types of oscillation groups, of which two (overexpressed type and repressed type) were considered arrhythmic due to the sharp increase or decrease in amplitude, respectively. For the rest of the tidal rhythmic transcripts, the harmonic group with stable amplitudes comprised 23.57% (n = 1,499 of 6,361) of transcripts and the forced group with amplified amplitudes comprised 24.65% (n = 1,568 of 6,361) of transcripts, whereas 51.78% (n = 3,294 of 6,361) of transcripts with reduced amplitudes were included in the damped group (Fig 3A).

Although there was a significantly amplified or reduced amplitude in at least 75% of tidal rhythmic transcripts, the period and phase of most tidal cycles were seemingly fixed. Interestingly, the whole tidal transcriptome exhibited an antiphased expression pattern with many transcripts reaching the peak at the same time. We then divided the tidal transcriptome into two clusters by gene expression using K-Means clustering (S3A and S3B Fig). Cluster 1 and 2 showed a generally antithetical gene expression pattern over time, and the phases were almost complementary in the tidal cycle (Fig 3B and 3C). This bimodal expression pattern is widely observed in the circadian rhythms of terrestrial organisms that experience transcriptional ‘rush hours’ preceding dawn and dusk, which is considered to assist in making preparations for the impending change in lighting [5, 6, 42]. Likewise, *S. leurokolos* could schedule its peak of tidal gene expression around high tide and low tide to provide intrinsic fitness, as observed in other marine organisms [43-45].

The rhythmicity of 3,837 transcripts in cluster 1 was relatively stable with almost equivalent amounts of modest forced, harmonic, and damped oscillations, whereas the 2,524 transcripts in cluster 2 were nearly occupied by damped oscillations that decreased obviously in amplitude, particularly during the second half of experiment. Considering the effects of raw gene expression on rhythmicity detection, we calculated the significance of transcript overlaps between subgroups categorized by the original trend or the oscillation type using Fisher's exact test, and found an extremely high association between the two (S2 Table). Indeed, there was seemingly a strong

correlation between trend directions and oscillation types (S3C Fig). In other words, a tidal transcript with a decreasing expression trend was more likely to have a reduced amplitude, and vice versa. This likelihood was extremely high in cluster 2 where over 94% of tidal transcripts with a downward trend were also damped. Since we isolated *S. leurokolos* shrimps from the hydrothermal vent and cultivated them under constant conditions for 72 hours, there were unsurprisingly considerable changes in the gene expression over time corresponding to transcriptional responses to potential stresses such as decompression. Therefore, the amplitude likely decreases as a byproduct of declining gene expression levels, especially for most transcripts in cluster 2. Although desynchronization between different tissues of *S. leurokolos* could lead to arrhythmic gene expression in our free-running study, we still detected a considerable number of rhythmic transcripts with highly synchronized expression, suggesting the effect of desynchronization was likely not significant.

Wide range of biological processes related to tidal cycles in *S. leurokolos*

The tidal rhythmic transcripts could be categorized by gene expression, oscillation types, and original trends, all of which included several subgroups that likely reflected similar or different biological relevance. To search for potential biological functions modulated by tidal rhythms, we performed functional enrichment analyses over the tidal transcriptome based on these three classification schemes using clusterProfiler [46]. Gene ontology (GO) and KEGG pathway analyses revealed that tidal rhythms generally affected various biological processes such as DNA repair, regulation of transcription, translation, transport, organelle organization, and citrate cycle (Fig 3D and S4 Fig). There was an expected high correlation between the biological functions of classified subgroups. For example, terms enriched in cluster 2 were more or less the same as those in the damped or downward subgroup. Notably, rhythmic processes related to the nucleus such as chromatin organization, DNA biosynthetic process, and transcription were uniquely enriched in cluster 1; whereas rhythmic processes supported by the cytoplasm such as translation, protein folding, vesicle-mediated transport, and oxidative phosphorylation were highly enriched in cluster 2. Thus, it is likely that *S. leurokolos* shrimps can organize various rhythmic biological processes in terms of spatial and temporal expression patterns to coordinate their internal physiology, regardless of the presence of clear zeitgebers.

In hydrothermal vents, particularly near the fluid orifice where *S. leurokolos* inhabits, hot, anoxic fluids with abundant potentially toxic chemical substances (e.g., hydrogen

sulfide) mix dramatically with the cold surrounding seawater, resulting in an extreme and variable environment. Vent organisms have evolved various adaptive strategies at morphological, physiological, and biochemical levels [19]. We hypothesized that intrinsic rhythms could help vent animals schedule their activities to cope with the harsh environment, and as expected, we found many transcripts related to various cellular stress response processes were tidally oscillated. These tidal oscillations include sulfide:quinone oxidoreductase (SQR), 3-mercaptopyruvate sulfurtransferase (3-MST) and sulfotransferases (SULTs) genes that play a key role in sulfur metabolism (Fig 4A) [47], together with catalase (CAT), superoxide dismutase (SOD), glutathione S-transferase (GST), glutathione peroxidase (GPX), and several enzymes from the Cytochrome P450 family, which are involved in the reactive oxygen species (ROS) homeostasis and cellular detoxification (Fig 4B) [48, 49]. In addition, tidal genes influence other cellular processes such as heat and hypoxia response, including heat shock proteins (HSPs), hypoxia up-regulated protein 1 (HYOU1), hypoxia-inducible factor 1-alpha inhibitor (FIH-1), egl nine homolog 1 (EGLN1) (Fig 4C). Most of these transcripts showed damped rhythmic expression over time under constant conditions, suggesting that *in situ* environmental cues were necessary for the maintenance and synchronization of rhythmic processes related to stress responses. In contrast, most tidal genes involved in the innate immune response of decapods, such as cathepsin L, relish, akirin 2, prophenoloxidase-activating factor (PPAFs), and a homolog of *Rimicaris exculata* (another alvinocaridid vent shrimp) C-type lectin 1, showed steady or amplified expression over time (Fig 4D) [50, 51]. The results reveal broad tidal regulation of gene expression in the cellular response to various environmental stresses, suggesting an adaptive advantage for *S. leurokolos* living in harsh, fluctuating environments.

Mounting evidence suggests the presence of cross-talking between circadian clocks and the cell cycle [52, 53]. Here, we found the annotation of many tidal transcripts was related to the cell cycle. The transition between G1 and S is controlled and regulated by key genes involved in the checkpoint pathways, of which several were tidally oscillating in the transcriptome, including cyclin D2, tumor suppressor protein p53, c-Myc binding protein 2 (MYCBP2), retinoblastoma-like protein 1 (RBL1), transcription factor E2F2 and E2F5, TIMELESS-interaction protein (TIPIN), and E3 ubiquitin-protein ligase MDM2 (S5A Fig) [52-55]. In addition, major components of the RAD9-RAD1-HUS1 clamp complex that play pivotal roles in DNA repair oscillate in the tidal range (S5B Fig) [56]. As crucial elements of the spindle assembly checkpoint (SAC), genes such as

mitotic arrest deficient 2 (MAD2), serine/threonine-protein kinase BUB1 and BUB3 that regulate chromosome separation were also found to be tidally cycling (S5C Fig) [57]. Taken together, tidal rhythms appear to generally regulate the progression of the cell cycle in *S. leurokolos* to cope with DNA damage derived from periodic intrinsic and environmental stresses.

Possible molecular basis and zeitgebers of biological rhythms in *S. leurokolos*

We reveal broad rhythmic gene expression of *S. leurokolos* under constant conditions, and many of the oscillations show a high stability of rhythmicity over several cycles, indicating the possible presence of endogenous oscillators that govern the dominant tidal rhythms in *S. leurokolos*. Based on circatidal locomotor and gene expression rhythms observed in various coastal and marine animals, two much-debated major hypotheses have been proposed to explain the molecular mechanisms underlying circatidal rhythms [58]. Generally, the circatidal rhythms could rely on either (a) an independent circatidal oscillator (a unimodal 12.4-hour clock [59] or two coupled unimodal antiphase 24.8-hour clocks [60]) that are not associated with the circadian clock or (b) a single bimodal clock that could transform rhythms between circatidal and circadian patterns depending on the dominant zeitgeber [61].

We searched for and identified *S. leurokolos* homologs of the canonical circadian clock genes that form the molecular oscillator in the fruitfly *Drosophila melanogaster*, including Clock, Period (PER), Timeless (TIM), Cryptochrome (CRY), Clockwork orange (CWO), Double-time (DBT, also known as casein kinase 1ε), Vrille (VRI), and PDP1ε [7] (S6A-D Fig). These well-conserved core clock components form a negative feedback loop containing transcriptional repressors Period and Timeless and transcriptional activators Clock and Bmal/Cycle. However, no Bmal/Cycle transcript was identified in *S. leurokolos* and the Clock transcript exhibited extremely low expression that rendered it unfeasible for rhythm analysis. Indeed, all *S. leurokolos* clock gene homologs lacked obvious 24-hour rhythmicity (Fig 5A-G). Although there was a possibility that some clock genes oscillated in certain tissues, and were detected as disorganized because of the desynchronization of expression from multiple tissues, we found a relatively low number of 24-hour oscillated transcripts in the temporal transcriptome of *S. leurokolos*. This may provide intrinsic fitness for these hydrothermal vent shrimps that are likely completely isolated from the surface as adults [62]. Moreover, most clock genes showed a lack of rhythmicity in the tidal range as well, except for Double-time, a kinase taking part in the post-translational modifications of

biological rhythms [63] (Fig 5E). The Period transcript tidally oscillated in the first half of the free-running experiment while becoming disordered and showing the opposite expression compared to the Timeless transcript in the second half (Fig 5A and 5B). Since a robust endogenous clock is required to be free-running with a self-sustained period for maintaining the rhythmicity of tidal oscillations in *S. leurokolos*, we hypothesize that there is a circatidal clock with independent molecular components from the circadian clocks. Separate circadian and circatidal clocks were also reported in the intertidal isopod *Eurydice pulchra* [64] and mangrove cricket *Apteronemobius asahinai* [65]. Nevertheless, the core clock genes still encode functional proteins with conserved domains (S6E Fig), and we cannot exclude the possibility that some core circadian clock genes are necessary for tidal rhythms [66, 67], even though they lose free-running transcription rhythmicity. These circadian clock genes may also be useful during the larval dispersal stage of the shrimp, which may take place in the photic zone [68].

Although *S. leurokolos* shrimps likely generate tidal rhythms using an endogenous circatidal clock, it is still difficult to understand and test how they synchronized their intrinsic rhythms given the highly variable environmental factors at their habitat. Temperature is likely not an appropriate zeitgeber due to the dramatic fluctuation with frequency at the seconds-minutes scale, which tends to disturb the entrainment. Moreover, the molecular heat stress response was observed to be rarely mobilized in the natural populations of alvinocaridid shrimps [28]. They choose to live in the thermal preferendum (10 to 25°C) most of the time and at the molecular level, are likely not sensitive to temperature changes [26]. As a phenotypic adaptation to the dark deep ocean, alvinocaridid shrimps such as *Rimicaris* and *Shinkaicaris* evolved a ‘dorsal eye’ instead of the externally differentiated eye [69]. Despite the lack of image-forming optics, this specialized organ is thought to be capable of detecting extremely dim light from the vent [70]. We then searched for phototransduction genes in *S. leurokolos*, including two main protein families, opsins and cryptochromes. We found a lack of light receptive-type cryptochrome transcript in *S. leurokolos*, but one transcript of transcriptional repressor-type cryptochrome involved in the regulation of the circadian clock showed a disordered expression (Fig 5C). For opsins, three transcripts were identified, including two middle wavelength-sensitive (MWS) opsins and one long wavelength-sensitive (LWS) opsin (S7 Fig). All three opsin transcripts were statistically arrhythmic, and quantitative PCR (qPCR) was performed to validate the results (Fig 5H-K). Therefore, potential light sources at vents, including thermal radiation from the chimney and

possible non-thermal emission mechanisms [71], are more likely to serve as a constant direction indicator to locate chimneys and therefore vent fluid, rather than acting as a principal zeitgeber for *S. leurokolos*. Given temperature and chemistry fluctuate dynamically, we suggest that food source [72, 73], pressure [74, 75], or even soundscape cues from the surface [76, 77] could be potentially useful zeitgebers for the deep-sea hydrothermal vent shrimp *S. leurokolos*.

Rhythmicity comparison of two vent species living in different microenvironments

A previous study on the Atlantic deep-sea hydrothermal vent mussel *Bathymodiolus azoricus* revealed *in situ* biological rhythms predominated by tidal gene expression [23], and here we report dominant free-running tidal rhythms in another vent species, *S. leurokolos*. Despite the different geographic localities of the two species, they both show similar biological rhythm patterns, likely reflecting a general influence of tidal modulations on deep-sea vent fauna.

From an ecological perspective, the plasticity of biological systems permits organisms to adjust their rhythms to cope with different environmental stresses [78]. For example, in the intertidal zone, high-shore animals exhibited more pronounced behavioral and transcriptional oscillations than the low-shore ones [43, 79]. In hydrothermal vents, local geochemical environments are important factors determining the micro-distribution of faunal assemblages, promoting vent organisms to evolve different adaptation strategies [80]. A long-term *in situ* monitoring revealed high stability in a *B. azoricus* mussel assemblage, and the temperature fluctuated mildly in both larger mussels (Mean ± SD = 6.2 ± 1.5□) and smaller mussels (5.0 ± 0.1□) [80]. However, *S. leurokolos* lives near the vent chimney, where the hot plume and cold surrounding seawater mix spontaneously, and the temperature fluctuates more dynamically at the seconds-minutes scale (Mean ± SD = 10.16 ± 1.71°C). Therefore, these two vent organisms likely evolved different strategies in biological rhythms to cope with their microenvironment variations.

To minimize the influence of rhythm analysis, we applied our transcriptome analysis and rhythm detection pipeline to the published *in situ* gene expression dataset of vent mussel *B. azoricus* [23]. Our analysis generated a total of 31,813 transcripts for rhythm detection analysis, which was near the number of contigs assembled in the published study (n = 34,196). As expected, rhythmic oscillations in the tidal range predominated the *in situ* temporal transcriptome of *B. azoricus*. Compared to *S. leurokolos*, however,

the proportion of tidal transcripts in the transcriptome was lower in *B. azoricus* regardless of the detection algorithm used (S8A and S8B Fig). Indeed, considering that rhythmic gene expression was organ-specific [5], the result was disputable as we detected overall rhythmicity within mixed tissues of *S. leurokolos*, whereas the study on *B. azoricus* only worked on gills. We further examined and compared the strength of tidal rhythms in the two species by calculating the rhythmicity index (RI) using the autocorrelation analysis, and the results suggested the general rhythmicity of tidal gene expression was greater in *S. leurokolos* (S8C Fig). This is unexpected since it should be easier for *B. azoricus*, living in a relatively distant area from the vent orifice with stable diffuse flow, to detect environmental factors influenced by tidal cycles. A possible explanation is that *S. leurokolos* needs to depend on a strong pacemaker to predict environmental fluctuations and prepare for transcriptional regulation, whereas *B. azoricus* could schedule the transcription by either relying on an endogenous clock or responding directly to the tidal-modulated environmental cues [23]. Why *S. leurokolos* inhabiting a more dynamic environment shows more robust rhythms compared to *B. azoricus* is an intriguing topic warranting future studies, although this could also be related to intrinsic differences between mussels and shrimps.

Conclusion

In this study, our analyses provide evidence for endogenous biological rhythms in the deep-sea hydrothermal vent shrimps *Shinkaicaris leurokolos* through a 72-hour free-running experiment and constrain the possible zeitgeber for biological clocks ticking in the deep, shedding light on biological rhythms in the light-absent biosphere (Fig 6). We propose that rhythms with a period of 24 hours driven by the conventional circadian clock largely decrease or even disappear in adult deep-sea hydrothermal vent fauna. Instead, rhythmic gene expression coordinated with approximately 12-hour tidal cycles, which are likely controlled by an independent circatidal clock, evolved as a temporal adaptation to the environmental fluctuations in hydrothermal ecosystems. Independent of solar energy but being influenced by tidal cycles, organisms in the deep sea may be powerful models for chronobiologists to decipher the evolution and molecular mechanisms of circatidal clocks, important across a wide range of living organisms.

Materials and methods

Environmental temperature monitoring

The local fluctuations in the temperature of a *Shinkaicaris leurokolos* colony on the NBC chimney (126°53.80'E, 27°47.45'N; 982 m deep) of the Original Site, Iheya North vent field were measured using a RINKO dissolved oxygen and temperature sensor (JFE Advantech Co., Ltd.) during dive #1610 of the remotely operated vehicle (ROV) *Hyper-Dolphin* on-board R/V *KAIYO* cruise KY14-01 for 162 seconds, and data were recorded every second. Published temperature data in a peripheral area of the original site, Iheya North vent field far away from active chimneys, which were recorded continuously every 10 min from the 4th of September 2010 to the 20th of August 2011, were re-analyzed [30]. We used the Lomb-Scargle periodogram to detect periodicity in the temperature time series.

Sampling procedure and experiment design

A total of 184 adult individuals of *Shinkaicaris leurokolos* were collected by a suction sampler from the top of the NBC chimney at the Original Site, Iheya North hydrothermal field during dive #1613 of ROV *Hyper-Dolphin* on-board R/V *KAIYO* during the cruise KY14-01. *S. leurokolos* were kept alive in a sealed temperature-insulated biobox, and transferred into total darkness under constant temperature (4°C) after recovery on-board. After 2.5 hours, five *S. leurokolos* individuals were collected by a meshed scoop, dissected and fixed every 4 hours for a total duration of 72 hours. During the sampling, we did not provide any food source as the previous laboratory study on behaviors of vent shrimps revealed that the introduction of food largely increased the activities of these shrimps [73]. As a possible zeitgeber [81], external food source gives an opportunity for shrimps to synchronize their activities and even gene expression at a certain time, which should be avoided in the free-running experiment. Despite that, *S. leurokolos* may feed on bacteria attached to other individuals. We did not find any dead shrimps during the sampling, which might reflect the health conditions of *S. leurokolos*. The cephalothorax and abdominal segments of each individual were preserved in RNAlater (Invitrogen), kept at 4°C overnight, and then stored at -80°C until RNA extraction.

RNA extraction and sequencing

Total RNA was extracted using TRIzol reagent (ThermoFisher) following the manufacturer's protocol. The quality of RNA was examined by 1% agarose gel electrophoresis. The mRNA from each shrimp tissue was enriched by Oligo-dT probes

and further reverse transcribed to first-strand cDNA for library construction. All cDNA libraries were sequenced on an Illumina NovaSeq 6000 platform with 150 bp paired-end mode.

De novo transcriptome assembly

A total of 57 RNA-Seq samples were generated from *S. leurokolos* during 72 hours of sampling at 4-hour intervals with three replicates per time point. Raw reads were firstly trimmed using Trimmomatic version 0.39 (set parameters: LEADING:10 TRAILING:10 SLIDINGWINDOW:4:15 MINLEN:50; [82]) in the paired-end mode, and then potentially associated bacteria contamination reads were removed with Kraken2 version 2.0.8-beta [83]. In the absence of an available genome reference of *S. leurokolos*, *de novo* assembly was performed with Trinity version 2.11.0 (set jaccard clip option; [84]). The transcripts with the highest expressed isoforms were kept. Salmon version 1.4.0 [85] was used to quantify the expression of each assembled transcript. Benchmarking Universal Single-Copy Orthologs (BUSCO) version 5.0.0 [86] was employed to evaluate the transcriptome completeness against the "metazoa_odb10" ortholog database.

Gene quantification and annotation

The Trimmed Means of M values (TMM) cross-sample normalization method [87] was applied to remove the sequencing variations and potential "batch effects" among samples using the abundance_estimates_to_matrix.pl script in the Trinity toolkit. The coding sequences were translated into proteins using TransDecoder version 5.5.0 (https://github.com/TransDecoder/TransDecoder) and only the single best open reading frame (ORF) was retained for each transcript. In addition, lowly expressed transcripts with 0 counts in at least 38 samples (i.e. two-thirds of all 57 samples) were filtered out, leaving 23,905 transcripts for subsequent analyses. The predicted proteins were annotated by searching the candidate protein sequences against the NCBI non-redundant (NR) database using BLASTP with DIAMOND version 2.0.13 [88] with ultra-sensitive mode and E-value threshold of 1×10^{-5}, the Kyoto Encyclopedia of Genes and Genomes (KEGG) database via KEGG Automatic Annotation Server (KAAS), and the Gene Ontology (GO) via BLAST2GO version 6.0 [89]. The gene enrichment analyses were performed with ClusterProfiler version 4.2.2 [46].

Gene expression analyses

The principle components analysis (PCA) was performed using the plotPCA function in R package DESeq2 version 1.34.0 [90]. Permutational multivariate analysis of variance

(PERMANOVA) and analysis of similarities (ANOSIM) were applied to test the statistical significance of the PCA results. The potential monotonic trends in the raw gene expression of all transcripts were determined with the Mann-Kendall trend test, and we pinpointed two overall clusters of transcripts that had either an upward trend (S score > 0 and *P*-value < 0.05) or a downward trend (S score < 0 and *P*-value < 0.05). To remove the trend and produce a steady baseline for subsequent rhythm analyses, we used CEEMDAN [25], an adaptive decomposition method designed for non-stationary and non-linear time series signals. The ceemdan detrend was performed with the R package Rlibeemd [91] (set parameters: num_imfs = 0; noise_strength = 0.4; S_number = 0; num_siftings = 50; ensemble_size = 250).

Rhythm detection analyses

Without benchmarking approaches for genome-scale analyses of biological rhythms [92, 93], we implemented the rhythmic analyses exploratorily under the considerations as follows: (a) choose the appropriate rhythm detection algorithms; (b) generate an overview of rhythmicity in our gene expression dataset using unbiased methods that can detect a wide range of periods; (c) detect the rhythmicity for each transcript using specialized methods with certain periods.

For *S. leurokolos*, we knew nothing about its biological rhythm, and no golden-standard circadian or non-circadian genes were available for evaluating the detection power (such as AUC values and ROC curves) of different algorithms [94, 95]. Thus, we assessed various rhythm detection methods based on our experiment design (for details see S1Table). Overall, we chose four rhythm detection algorithms in this study, the mathematic method eigenvalue/pencil [35] (carried out with customized scripts), the Extended Circadian Harmonic Oscillator application (ECHO; [36]), and two non-parametric statistical methods RAIN [38] and empirical JTK_CYCLE (eJTK; [39]), which were designed to detect asymmetric waveforms. For eigenvalue/pencil and ECHO, rhythmic transcripts with the periodicity of 10-14 hours and 22-26 hours were considered as tidal and daily oscillated [44]. Oscillations with the largest amplitude in one transcript for eigenvalue/pencil were considered the dominant oscillation [37]. For RAIN and eJTK, rhythmic transcripts with the periodicity of 12 hours and 24 hours were considered as tidal and daily cycling. Multiple-testing was carried out to adjust *P*-values using the Benjamini-Hochberg method for RAIN and ECHO, and an empirical method based on the gamma distribution for combining dependent *P*-values for eJTK. Transcripts with an FDR ≤ 0.05 were considered statistically rhythmic. The amplitude and Rhythmicity

Index (RI) of rhythmic transcripts were calculated by LimoRhyde2 [96] and autocorrelation analysis, respectively. Significance of amplitude and detected *P*-values between tidal and daily oscillations was examined with the unpaired Student's *t*-test, while the paired Student's *t*-test was conducted on the tidal and daily component of rhythmic transcripts. We also used ECHO to fit data with an extended fixed amplitude model and categorize the oscillation type using amplitude change coefficient (γ) as forced ($-0.15 < \gamma < -0.03$; amplified amplitude), harmonic ($-0.03 \leq \gamma \leq 0.03$; steady amplitude), damped ($0.03 < \gamma < 0.15$; reduced amplitude), overexpressed ($\gamma \leq -0.15$), and repressed ($\gamma > 0.15$), of which the latter two are considered arrhythmic [36]. The significance of overlaps between rhythmic transcripts with different original trends and oscillation types was examined using Fisher's exact test.

For the clustering of circatidal transcripts, we assessed four different clustering methods with different numbers of clusters by validation measures using the R package clVaild version 0.7 [97] and found the kmeans method with two clusters was estimated to be the most optimal one. Heatmaps were drawn with ComplexHeatmap version 2.10.0 [98] on Z-score normalized expression. All analyses and plots were performed in R version 4.1.1, except for eJTK which was performed using Python version 2.7.

Identification of putative circadian clock genes

We searched for putative circadian clock genes in our *de novo* assembled transcriptome using the proteic Basic Local Alignment Search Tool (BLASTP) carried out by DIAMOND with a series of known core clock and clock-associated genes as queries. For candidate circadian clock transcripts, sequences were scanned against the coding regions and conserved functional domains using the InterProScan tools [99]. To determine the sequence homology of candidate transcripts, we further conducted the phylogenetic analysis. The amino acid sequences were first aligned using MAFFT version 7.490 [100] and then trimmed using trimAl version 1.4.1 with the '-automated1' option [101]. The maximum-likelihood trees were then constructed using the IQ-Tree version 2.1.3 [102] with the ultrafast bootstrap approximation (UFBoot) and ModelFinder for examining the best-fit model. Overall, we reconstructed four phylogenetic trees by using the Q.insect+G4 model for the Clock and Bmal/Cycle tree, the Q.insect+I+G4 model for the Period tree and the Timeless/Timeout tree, and the LG+R4 model for the Photolyase/Cryptochrome tree. In the identified circadian clock genes, the Clock transcript exhibited extremely low expression and was thus excluded from the rhythm detection. Visualization of all phylogenetic trees was performed with

ggtree version 3.8.2 [103].

Quantitative PCR (qPCR) and phylogenetic analysis of opsin genes

To validate the gene expression levels deduced in the sequencing-based transcriptome analysis, we also performed qPCR analysis on one target gene (*opsin*) and one gene (*tubulin*) that serves as the internal standard in qPCR. In brief, the extracted RNA was treated with DNAse I (Invitrogen), and sequentially reverse-transcribed into single-strand cDNA by using the high-capacity cDNA reverse transcription kit (Applied Biosystems). QPCR was performed on A LightCycler 480 instrument II (Roche), and the relative gene expression level was analyzed based on the $2^{-\Delta\Delta Ct}$ method.

Their primer sequences are listed below:

>Tubulin_F

AACACGGCATTGAACCAACC

>Tubulin_R

CTATCCATTGTCCCCGGCTC

>Opsin_F

GCATCCTCGACTCCTGTAGC

>Opsin_R

CACGCATGGCTTTTTCGTGA

As it was unclear about the maximum absorption of identified opsin genes, a phylogenetic analysis was used to show the genealogy of the opsins of *S. leurokolos* together with other arthropod opsins. We collected a total of 94 opsin sequences from arthropods (including crustaceans, chelicerates, and insects), together with 5 vertebrate opsin clade sequences as an outgroup. The phylogenetic analysis was performed with the same procedure in the identification of candidate circadian clock genes. The maximum-likelihood phylogeny was finally built using IQ-Tree with 1000 replicates of the ultrafast bootstrap and LG+F+G5 model as the suggested best-fit model [102].

Acknowledgments

We are grateful to the ship captain and crews of R/V *KAIYO* as well as pilots and the technical team of ROV *Hyper-Dolphin* for their great efforts during sample collection during cruise KY14-01 led by Ken Takai (JAMSTEC). Hiroyuki Yamamoto, Shinsuke Kawagucci, and Hiromi K. Watanabe (JAMSTEC) are thanked for providing raw data of the temperature probe recordings published in [30].

Funding

Science and Technology Innovation Project of Laoshan Laboratory (LSKJ202203104)
Fundamental Research Funds for the Central Universities (202172002 and 202241002)
Young Taishan Scholars Program of Shandong Province (tsqn202103036)
Principal investigator projects of the Southern Marine Science and Engineering Guangdong Laboratory (Guangzhou) (2021HJ01)
Major Basic and Applied Research Projects of Guangdong Province (2019B030302004-04)
Southern Marine Science and Engineering Guangdong Laboratory (Guangzhou) (SMSEGL20SC01)
Hong Kong Special Administrative Region government (16101822, C2013-22GF)

Author contributions

Conceptualization: JS, TY, NM, and CC
Methodology: TY, NM, CC, and HYZ
Formal Analysis: HYZ and JS
Investigation: TY, CC
Writing – Original Draft: HYZ
Writing – Review & Editing: JS, CC
Visualization: HYZ and QQJ
Supervision: JS and TY
Project Administration: JS, P-YQ and TY
Funding Acquisition: JS and P-YQ

Competing interests

The authors declare that they have no competing interests.

Data and materials availability

Raw RNA-Seq data are available on NCBI as BioProject PRJNA993859. The *de novo* reference transcriptome of *Shinkaicaris leurokolos* is available in figshare (https://doi.org/10.6084/m9.figshare.23667327.v2). All original codes used in this work are available at GitHub (https://github.com/belphe/Shinkaicaris).

References

1. Panda S, Hogenesch JB, Kay SA. Circadian rhythms from flies to human. Nature. 2002;417(6886):329-35. doi: 10.1038/417329a.

2. Edgar RS, Green EW, Zhao Y, van Ooijen G, Olmedo M, Qin X, et al. Peroxiredoxins are conserved markers of circadian rhythms. Nature. 2012;485(7399):459-64. doi: 10.1038/nature11088.

3. Kondo T, Mori T, Lebedeva NV, Aoki S, Ishiura M, Golden SS. Circadian Rhythms in Rapidly Dividing Cyanobacteria. Science. 1997;275(5297):224-7. doi: doi:10.1126/science.275.5297.224.

4. Stoleru D, Peng Y, Agosto J, Rosbash M. Coupled oscillators control morning and evening locomotor behaviour of Drosophila. Nature. 2004;431(7010):862-8. doi: 10.1038/nature02926.

5. Zhang R, Lahens NF, Ballance HI, Hughes ME, Hogenesch JB. A circadian gene expression atlas in mammals: Implications for biology and medicine. Proceedings of the National Academy of Sciences. 2014;111(45):16219-24. doi: doi:10.1073/pnas.1408886111.

6. Mure LS, Le HD, Benegiamo G, Chang MW, Rios L, Jillani N, et al. Diurnal transcriptome atlas of a primate across major neural and peripheral tissues. Science. 2018;359(6381):eaao0318. doi: doi:10.1126/science.aao0318.

7. Patke A, Young MW, Axelrod S. Molecular mechanisms and physiological importance of circadian rhythms. Nature Reviews Molecular Cell Biology. 2020;21(2):67-84. doi: 10.1038/s41580-019-0179-2.

8. Beale AD, Whitmore D, Moran D. Life in a dark biosphere: a review of circadian physiology in "arrhythmic" environments. J Comp Physiol B. 2016;186(8):947-68. Epub 2016/06/04. doi: 10.1007/s00360-016-1000-6. PubMed PMID: 27263116.

9. Abhilash L, Shindey R, Sharma VK. To be or not to be rhythmic? A review of studies on organisms inhabiting constant environments. Biological Rhythm Research. 2017;48(5):677-91. doi: 10.1080/09291016.2017.1345426.

10. Ramirez-Llodra E, Brandt A, Danovaro R, De Mol B, Escobar E, German CR, et al. Deep, diverse and definitely different: unique attributes of the world's largest ecosystem. Biogeosciences. 2010;7(9):2851-99. doi: 10.5194/bg-7-2851-2010.

11. Aguzzi J, Company JB, Costa C, Menesatti P, Garcia JA, Bahamon N, et al. Activity rhythms in the deep-sea: a chronobiological approach. FBL. 2011;16(1):131-50. doi: 10.2741/3680.

12. Warrant EJ, Locket NA. Vision in the deep sea. Biological Reviews.

2004;79(3):671-712. doi: https://doi.org/10.1017/S1464793103006420.

13. Aguzzi J, Costa C, Furushima Y, Chiesa JJ, Company JB, Menesatti P, et al. Behavioral rhythms of hydrocarbon seep fauna in relation to internal tides. Marine Ecology Progress Series. 2010;418:47-56.

14. Aguzzi J, Company JB, Costa C, Menesatti P, Garcia JA, Bahamon N, et al. Activity rhythms in the deep-sea: a chronobiological approach. Front Biosci (Landmark Ed) [Internet]. 2011 2011/01//; 16:[131-50 pp.]. Available from: http://europepmc.org/abstract/MED/21196163

https://doi.org/10.2741/3680.

15. Chevaldonné P, Desbruyères D, Ha?Tre ML. Time-series of temperature from three deep-sea hydrothermal vent sites. Deep Sea Research Part A Oceanographic Research Papers. 1991;38(11):1417-30.

16. Tivey MK, Bradley AM, Joyce TM, Kadko D. Insights into tide-related variability at seafloor hydrothermal vents from time-series temperature measurements. Earth and Planetary Science Letters. 2002;202(3):693-707. doi: https://doi.org/10.1016/S0012-821X(02)00801-4.

17. Crone TJ, Wilcock WSD. Modeling the effects of tidal loading on mid-ocean ridge hydrothermal systems. Geochemistry, Geophysics, Geosystems. 2005;6(7). doi: https://doi.org/10.1029/2004GC000905.

18. Barreyre T, Escartín J, Sohn RA, Cannat M, Ballu V, Crawford WC. Temporal variability and tidal modulation of hydrothermal exit-fluid temperatures at the Lucky Strike deep-sea vent field, Mid-Atlantic Ridge. Journal of Geophysical Research: Solid Earth. 2014;119(4):2543-66. doi: https://doi.org/10.1002/2013JB010478.

19. Childress JJ, Fisher CR. The biology of hydrothermal vent animals: physiology, biochemistry, and autotrophic symbioses. Oceanography and Marine Biology. 1992;30:337-441.

20. Nedoncelle K, Lartaud F, de Rafelis M, Boulila S, Le Bris N. A new method for high-resolution bivalve growth rate studies in hydrothermal environments. Marine Biology. 2013;160(6):1427-39. doi: 10.1007/s00227-013-2195-7.

21. Cuvelier D, Legendre P, Laes A, Sarradin P-M, Sarrazin J. Rhythms and Community Dynamics of a Hydrothermal Tubeworm Assemblage at Main Endeavour Field – A Multidisciplinary Deep-Sea Observatory Approach. PLOS ONE. 2014;9(5):e96924. doi: 10.1371/journal.pone.0096924.

22. Cuvelier D, Legendre P, Laës-Huon A, Sarradin PM, Sarrazin J. Biological and environmental rhythms in (dark) deep-sea hydrothermal ecosystems. Biogeosciences. 2017;14(12):2955-77. doi: 10.5194/bg-14-2955-2017.

23. Mat AM, Sarrazin J, Markov GV, Apremont V, Dubreuil C, Eché C, et al. Biological rhythms in the deep-sea hydrothermal mussel Bathymodiolus azoricus. Nature Communications. 2020;11(1):3454. doi: 10.1038/s41467-020-17284-4.

24. Watanabe H, Kojima S. Vent Fauna in the Okinawa Trough. In: Ishibashi J-i, Okino K, Sunamura M, editors. Subseafloor Biosphere Linked to Hydrothermal Systems: TAIGA Concept. Tokyo: Springer Japan; 2015. p. 449-59.

25. Yahagi T, Watanabe H, Ishibashi J, Kojima S. Genetic population structure of four hydrothermal vent shrimp species (Alvinocarididae) in the Okinawa Trough, Northwest Pacific. Marine Ecology Progress Series. 2015;529:159-69.

26. Ravaux J, Cottin D, Chertemps T, Hamel G, Shillito B. Hydrothermal vent shrimps display low expression of the heat-inducible hsp70 gene in nature. Marine Ecology Progress Series. 2009;396:153-6.

27. Cottin D, Shillito B, Chertemps T, Tanguy A, Léger N, Ravaux J. Identification of differentially expressed genes in the hydrothermal vent shrimp Rimicaris exoculata exposed to heat stress. Marine Genomics. 2010;3(2):71-8. doi: https://doi.org/10.1016/j.margen.2010.05.002.

28. Ravaux J, Léger N, Hamel G, Shillito B. Assessing a species thermal tolerance through a multiparameter approach: the case study of the deep-sea hydrothermal vent shrimp Rimicaris exoculata. Cell Stress and Chaperones. 2019;24(3):647-59. doi: 10.1007/s12192-019-01003-0.

29. Helm B, Stevenson TJ. Annual, Lunar, and Tidal Clocks: Annual, Lunar, and Tidal Clocks; 2014.

30. Kawagucci S, Miyazaki J, Nakajima R, Nozaki T, Takaya Y, Kato Y, et al. Post-drilling changes in fluid discharge pattern, mineral deposition, and fluid chemistry in the Iheya North hydrothermal field, Okinawa Trough. Geochemistry, Geophysics, Geosystems. 2013;14(11):4774-90. doi: https://doi.org/10.1002/2013GC004895.

31. JOHNSON KS, BEEHLER CL, SAKAMOTO-ARNOLD CM, CHILDRESS JJ. In Situ Measurements of Chemical Distributions in a Deep-Sea Hydrothermal Vent Field. Science. 1986;231(4742):1139-41. doi: 10.1126/science.231.4742.1139.

32. Strauss J, Dircksen H. Circadian clocks in crustaceans: identified neuronal and cellular systems. Frontiers in bioscience. 2010;15(1):1040-74.

33. Torres ME, Colominas MA, Schlotthauer G, Flandrin P, editors. A complete ensemble empirical mode decomposition with adaptive noise. 2011 IEEE International Conference on Acoustics, Speech and Signal Processing (ICASSP); 2011 22-27 May 2011.

34. Muratore D, Boysen AK, Harke MJ, Becker KW, Casey JR, Coesel SN, et al.

Complex marine microbial communities partition metabolism of scarce resources over the diel cycle. Nature Ecology & Evolution. 2022. doi: 10.1038/s41559-021-01606-w.

35. Zhu B, Zhang Q, Pan Y, Mace EM, York B, Antoulas AC, et al. A Cell-Autonomous Mammalian 12 hr Clock Coordinates Metabolic and Stress Rhythms. Cell Metabolism. 2017;25(6):1305-19.e9. doi: https://doi.org/10.1016/j.cmet.2017.05.004.

36. De los Santos H, Collins EJ, Mann C, Sagan AW, Jankowski MS, Bennett KP, et al. ECHO: an application for detection and analysis of oscillators identifies metabolic regulation on genome-wide circadian output. Bioinformatics. 2019;36(3):773-81. doi: 10.1093/bioinformatics/btz617.

37. Pan Y, Ballance H, Meng H, Gonzalez N, Kim S-M, Abdurehman L, et al. 12-h clock regulation of genetic information flow by XBP1s. PLOS Biology. 2020;18(1):e3000580. doi: 10.1371/journal.pbio.3000580.

38. Thaben PF, Westermark PO. Detecting Rhythms in Time Series with RAIN. Journal of Biological Rhythms. 2014;29(6):391-400. doi: 10.1177/0748730414553029. PubMed PMID: 25326247.

39. Hutchison AL, Maienschein-Cline M, Chiang AH, Tabei SMA, Gudjonson H, Bahroos N, et al. Improved Statistical Methods Enable Greater Sensitivity in Rhythm Detection for Genome-Wide Data. PLOS Computational Biology. 2015;11(3):e1004094. doi: 10.1371/journal.pcbi.1004094.

40. Santos HDl, Collins EJ, Hurley JM, Bennett KP. Circadian Rhythms in Neurospora Exhibit Biologically Relevant Driven and Damped Harmonic Oscillations. Proceedings of the 8th ACM International Conference on Bioinformatics, Computational Biology,and Health Informatics; Boston, Massachusetts, USA: Association for Computing Machinery; 2017. p. 455–63.

41. Yamazaki S, Numano R, Abe M, Hida A, Takahashi R-i, Ueda M, et al. Resetting Central and Peripheral Circadian Oscillators in Transgenic Rats. Science. 2000;288(5466):682-5. doi: doi:10.1126/science.288.5466.682.

42. Taton A, Erikson C, Yang Y, Rubin BE, Rifkin SA, Golden JW, et al. The circadian clock and darkness control natural competence in cyanobacteria. Nature Communications. 2020;11(1):1688. doi: 10.1038/s41467-020-15384-9.

43. Gracey AY, Chaney ML, Boomhower JP, Tyburczy WR, Connor K, Somero GN. Rhythms of Gene Expression in a Fluctuating Intertidal Environment. Current Biology. 2008;18(19):1501-7. doi: https://doi.org/10.1016/j.cub.2008.08.049.

44. Connor KM, Gracey AY. Circadian cycles are the dominant transcriptional rhythm in the intertidal mussel <em>Mytilus californianus</em&gt. Proceedings of the National Academy of Sciences. 2011;108(38):16110. doi: 10.1073/pnas.1111076108.

45. Satoh A, Terai Y. Circatidal gene expression in the mangrove cricket Apteronemobius asahinai. Scientific Reports. 2019;9(1):3719. doi: 10.1038/s41598-019-40197-2.

46. Wu T, Hu E, Xu S, Chen M, Guo P, Dai Z, et al. clusterProfiler 4.0: A universal enrichment tool for interpreting omics data. The Innovation. 2021;2(3):100141. doi: https://doi.org/10.1016/j.xinn.2021.100141.

47. Tobler M, Passow CN, Greenway R, Kelley JL, Shaw JH. The Evolutionary Ecology of Animals Inhabiting Hydrogen Sulfide–Rich Environments. Annual Review of Ecology, Evolution, and Systematics. 2016;47(1):239-62. doi: 10.1146/annurev-ecolsys-121415-032418.

48. Zhang J, Sun Q-l, Luan Z-d, Lian C, Sun L. Comparative transcriptome analysis of Rimicaris sp. reveals novel molecular features associated with survival in deep-sea hydrothermal vent. Scientific Reports. 2017;7(1):2000. doi: 10.1038/s41598-017-02073-9.

49. Hui M, Cheng J, Sha Z. Adaptation to the deep-sea hydrothermal vents and cold seeps: Insights from the transcriptomes of Alvinocaris longirostris in both environments. Deep Sea Research Part I: Oceanographic Research Papers. 2018;135:23-33. doi: https://doi.org/10.1016/j.dsr.2018.03.014.

50. Wang G, Lei Y, Kang T, Li Z, Fei H, Zeng B, et al. Two C-type lectins (ReCTL-1, ReCTL-2) from Rimicaris exoculata display broad nonself recognition spectrum with novel carbohydrate binding specificity. Fish & Shellfish Immunology. 2020;96:152-60. doi: https://doi.org/10.1016/j.fsi.2019.11.068.

51. Kulkarni A, Krishnan S, Anand D, Kokkattunivarthil Uthaman S, Otta SK, Karunasagar I, et al. Immune responses and immunoprotection in crustaceans with special reference to shrimp. Reviews in Aquaculture. 2021;13(1):431-59. doi: https://doi.org/10.1111/raq.12482.

52. Hunt T, Sassone-Corsi P. Riding Tandem: Circadian Clocks and the Cell Cycle. Cell. 2007;129(3):461-4. doi: https://doi.org/10.1016/j.cell.2007.04.015.

53. Farshadi E, van der Horst GTJ, Chaves I. Molecular Links between the Circadian Clock and the Cell Cycle. Journal of Molecular Biology. 2020;432(12):3515-24. doi: https://doi.org/10.1016/j.jmb.2020.04.003.

54. Yoshizawa-Sugata N, Masai H. Human Tim/Timeless-interacting Protein, Tipin, Is Required for Efficient Progression of S Phase and DNA Replication Checkpoint *. Journal of Biological Chemistry. 2007;282(4):2729-40. doi: 10.1074/jbc.M605596200.

55. Masri S, Cervantes M, Sassone-Corsi P. The circadian clock and cell cycle: interconnected biological circuits. Current Opinion in Cell Biology. 2013;25(6):730-4. doi: https://doi.org/10.1016/j.ceb.2013.07.013.

56. Bermudez VP, Lindsey-Boltz LA, Cesare AJ, Maniwa Y, Griffith JD, Hurwitz J, et al. Loading of the human 9-1-1 checkpoint complex onto DNA by the checkpoint clamp loader hRad17-replication factor C complex *in vitro*. Proceedings of the National Academy of Sciences. 2003;100(4):1633-8. doi: doi:10.1073/pnas.0437927100.

57. Klebig C, Korinth D, Meraldi P. Bub1 regulates chromosome segregation in a kinetochore-independent manner. Journal of Cell Biology. 2009;185(5):841-58. doi: 10.1083/jcb.200902128.

58. Häfker NS, Andreatta G, Manzotti A, Falciatore A, Raible F, Tessmar-Raible K. Rhythms and Clocks in Marine Organisms. Annual Review of Marine Science. 2023;15(1):null. doi: 10.1146/annurev-marine-030422-113038. PubMed PMID: 36028229.

59. Naylor E. Crab Clockwork: The Case for Interactive Circatidal and Circadian Oscillators Controlling Rhythmic Locomotor Activity of Carcinus Maenas. Chronobiology International. 1996;13(3):153-61. doi: 10.3109/07420529609012649.

60. Palmer JD. Review of the Dual-Clock Control of Tidal Rhythms and the Hypothesis that the Same Clock Governs Both Circatidal and Circadian Rhythms. Chronobiology International. 1995;12(5):299-310. doi: 10.3109/07420529509057279.

61. Enright JT. Plasticity in an isopod's clockworks: Shaking shapes form and affects phase and frequency. Journal of comparative physiology. 1976;107(1):13-37. doi: 10.1007/BF00663916.

62. Methou P, Chen C, Kayama Watanabe H, Cambon M-A, Pradillon F. Reproduction in deep-sea vent shrimps is influenced by diet, with rhythms apparently unlinked to surface production. Ecology and Evolution. 2022;12(7):e9076. doi: https://doi.org/10.1002/ece3.9076.

63. Parnell AA, De Nobrega AK, Lyons LC. Translating around the clock: Multi-level regulation of post-transcriptional processes by the circadian clock. Cellular Signalling. 2021;80:109904. doi: https://doi.org/10.1016/j.cellsig.2020.109904.

64. Zhang L, Hastings Michael H, Green Edward W, Tauber E, Sladek M, Webster Simon G, et al. Dissociation of Circadian and Circatidal Timekeeping in the Marine Crustacean Eurydice pulchra. Current Biology. 2013;23(19):1863-73. doi: https://doi.org/10.1016/j.cub.2013.08.038.

65. Takekata H, Numata H, Shiga S, Goto SG. Silencing the circadian clock gene Clock using RNAi reveals dissociation of the circatidal clock from the circadian clock in the mangrove cricket. Journal of Insect Physiology. 2014;68:16-22. doi: https://doi.org/10.1016/j.jinsphys.2014.06.012.

66. Zhang L, Green EW, Webster SG, Hastings MH, Wilcockson DC, Kyriacou CP. The circadian clock gene bmal1 is necessary for co-ordinated circatidal rhythms

in the marine isopod Eurydice pulchra (Leach). bioRxiv. 2022:2022.12.21.521378. doi: 10.1101/2022.12.21.521378.

67. Kwiatkowski ER, Schnytzer Y, Rosenthal JJ, Emery P. Behavioral circatidal rhythms require Bmal1 in Parhyale hawaiensis. Current Biology. 2023.

68. Yahagi T, Kayama Watanabe H, Kojima S, Kano Y. Do larvae from deep-sea hydrothermal vents disperse in surface waters? Ecology. 2017;98(6):1524-34. doi: https://doi.org/10.1002/ecy.1800.

69. Komai T, Chan T-Y. A new genus and two new species of alvinocaridid shrimps (Crustacea: Decapoda: Caridea) from a hydrothermal vent field off northeastern Taiwan. Zootaxa. 2010;2372(1):15–32. doi: 10.11646/zootaxa.2372.1.3.

70. Dover CLV, Szuts EZ, Chamberlain SC, Cann JR. A novel eye in 'eyeless' shrimp from hydrothermal vents of the Mid-Atlantic Ridge. Nature. 1989;337(6206):458-60. doi: 10.1038/337458a0.

71. Van Dover CL, Reynolds GT, Chave AD, Tyson JA. Light at deep-sea hydrothermal vents. Geophysical Research Letters. 1996;23(16):2049-52. doi: https://doi.org/10.1029/96GL02151.

72. Williams BG, Pilditch CA. The Entrainment of Persistent Tidal Rhythmicity in a Filter-Feeding Bivalve Using Cycles of Food Availability. Journal of Biological Rhythms. 1997;12(2):173-81. doi: 10.1177/074873049701200208. PubMed PMID: 9090570.

73. Matabos M, Cuvelier D, Brouard J, Shillito B, Ravaux J, Zbinden M, et al. Behavioural study of two hydrothermal crustacean decapods: Mirocaris fortunata and Segonzacia mesatlantica, from the Lucky Strike vent field (Mid-Atlantic Ridge). Deep Sea Research Part II: Topical Studies in Oceanography. 2015;121:146-58. doi: https://doi.org/10.1016/j.dsr2.2015.04.008.

74. Reid DG, Naylor E. Entrainment of Bimodal Circatidal Rhythms in the Shore Crab Carcinus maenas. Journal of Biological Rhythms. 1990;5(4):333-47. doi: 10.1177/074873049000500405. PubMed PMID: 2133140.

75. Akiyama T. Entrainment of the Circatidal Swimming Activity Rhythm in the Cumacean Dimorphostylis asiatica (Crustacea) to 12.5-hour Hydrostatic Pressure Cycles. Zoological Science. 2004;21(1):29-38, 10.

76. Crone TJ, Wilcock WSD, Barclay AH, Parsons JD. The Sound Generated by Mid-Ocean Ridge Black Smoker Hydrothermal Vents. PLOS ONE. 2006;1(1):e133. doi: 10.1371/journal.pone.0000133.

77. Lin T-H, Kawagucci S. Acoustic twilight: A year-long seafloor monitoring unveils phenological patterns in the abyssal soundscape. Limnology and Oceanography Letters. 2024;n/a(n/a). doi: https://doi.org/10.1002/lol2.10358.

78. Helm B, Visser ME, Schwartz W, Kronfeld-Schor N, Gerkema M, Piersma T, et al. Two sides of a coin: ecological and chronobiological perspectives of timing in the wild. Philosophical Transactions of the Royal Society B: Biological Sciences. 2017;372(1734):20160246. doi: doi:10.1098/rstb.2016.0246.

79. Miller LP, Dowd WW. Multimodal in situ datalogging quantifies inter-individual variation in thermal experience and persistent origin effects on gaping behavior among intertidal mussels (Mytilus californianus). Journal of Experimental Biology. 2017;220(22):4305-19. doi: 10.1242/jeb.164020.

80. Van Audenhaege L, Matabos M, Brind'Amour A, Drugmand J, Laës-Huon A, Sarradin P-M, et al. Long-term monitoring reveals unprecedented stability of a vent mussel assemblage on the Mid-Atlantic Ridge. Progress in Oceanography. 2022;204:102791. doi: https://doi.org/10.1016/j.pocean.2022.102791.

81. Stephan FK. The “Other” Circadian System: Food as a Zeitgeber. Journal of Biological Rhythms. 2002;17(4):284-92. doi: 10.1177/074873040201700402. PubMed PMID: 12164245.

82. Bolger AM, Lohse M, Usadel B. Trimmomatic: a flexible trimmer for Illumina sequence data. Bioinformatics. 2014;30(15):2114-20. doi: 10.1093/bioinformatics/btu170.

83. Wood DE, Lu J, Langmead B. Improved metagenomic analysis with Kraken 2. Genome Biology. 2019;20(1):257. doi: 10.1186/s13059-019-1891-0.

84. Grabherr MG, Haas BJ, Yassour M, Levin JZ, Thompson DA, Amit I, et al. Full-length transcriptome assembly from RNA-Seq data without a reference genome. Nature Biotechnology. 2011;29(7):644-52. doi: 10.1038/nbt.1883.

85. Patro R, Duggal G, Love MI, Irizarry RA, Kingsford C. Salmon provides fast and bias-aware quantification of transcript expression. Nature Methods. 2017;14(4):417-9. doi: 10.1038/nmeth.4197.

86. Manni M, Berkeley MR, Seppey M, Simão FA, Zdobnov EM. BUSCO Update: Novel and Streamlined Workflows along with Broader and Deeper Phylogenetic Coverage for Scoring of Eukaryotic, Prokaryotic, and Viral Genomes. Molecular Biology and Evolution. 2021;38(10):4647-54. doi: 10.1093/molbev/msab199.

87. Robinson MD, Oshlack A. A scaling normalization method for differential expression analysis of RNA-seq data. Genome Biology. 2010;11(3):R25. doi: 10.1186/gb-2010-11-3-r25.

88. Buchfink B, Reuter K, Drost H-G. Sensitive protein alignments at tree-of-life scale using DIAMOND. Nature Methods. 2021;18(4):366-8. doi: 10.1038/s41592-021-01101-x.

89. Conesa A, Götz S, García-Gómez JM, Terol J, Talón M, Robles M. Blast2GO: a universal tool for annotation, visualization and analysis in functional genomics research. Bioinformatics. 2005;21(18):3674-6. doi: 10.1093/bioinformatics/bti610.

90. Love MI, Huber W, Anders S. Moderated estimation of fold change and dispersion for RNA-seq data with DESeq2. Genome Biology. 2014;15(12):550. doi: 10.1186/s13059-014-0550-8.

91. Luukko PJJ, Helske J, Räsänen E. Introducing libeemd: a program package for performing the ensemble empirical mode decomposition. Computational Statistics. 2016;31(2):545-57. doi: 10.1007/s00180-015-0603-9.

92. Hughes ME, Abruzzi KC, Allada R, Anafi R, Arpat AB, Asher G, et al. Guidelines for Genome-Scale Analysis of Biological Rhythms. Journal of Biological Rhythms. 2017;32(5):380-93. doi: 10.1177/0748730417728663. PubMed PMID: 29098954.

93. Li J, Grant GR, Hogenesch JB, Hughes ME. Chapter Sixteen - Considerations for RNA-seq Analysis of Circadian Rhythms. In: Sehgal A, editor. Methods in Enzymology. 551: Academic Press; 2015. p. 349-67.

94. Laloum D, Robinson-Rechavi M. Methods detecting rhythmic gene expression are biologically relevant only for strong signal. PLOS Computational Biology. 2020;16(3):e1007666. doi: 10.1371/journal.pcbi.1007666.

95. Mei W, Jiang Z, Chen Y, Chen L, Sancar A, Jiang Y. Genome-wide circadian rhythm detection methods: systematic evaluations and practical guidelines. Briefings in Bioinformatics. 2020;22(3):bbaa135. doi: 10.1093/bib/bbaa135.

96. Obodo D, Outland EH, Hughey JJ. LimoRhyde2: genomic analysis of biological rhythms based on effect sizes. bioRxiv. 2023:2023.02.02.526897. doi: 10.1101/2023.02.02.526897.

97. Brock G, Pihur V, Datta S, Datta S. clValid: An R Package for Cluster Validation. Journal of Statistical Software. 2008;25(4):1 - 22. doi: 10.18637/jss.v025.i04.

98. Gu Z, Eils R, Schlesner M. Complex heatmaps reveal patterns and correlations in multidimensional genomic data. Bioinformatics. 2016;32(18):2847-9. doi: 10.1093/bioinformatics/btw313.

99. Jones P, Binns D, Chang H-Y, Fraser M, Li W, McAnulla C, et al. InterProScan 5: genome-scale protein function classification. Bioinformatics. 2014;30(9):1236-40. doi: 10.1093/bioinformatics/btu031.

100. Katoh K, Standley DM. MAFFT Multiple Sequence Alignment Software Version 7: Improvements in Performance and Usability. Molecular Biology and Evolution. 2013;30(4):772-80. doi: 10.1093/molbev/mst010.

101. Capella-Gutiérrez S, Silla-Martínez JM, Gabaldón T. trimAl: a tool for

automated alignment trimming in large-scale phylogenetic analyses. Bioinformatics. 2009;25(15):1972-3. doi: 10.1093/bioinformatics/btp348.

102. Minh BQ, Schmidt HA, Chernomor O, Schrempf D, Woodhams MD, von Haeseler A, et al. IQ-TREE 2: New Models and Efficient Methods for Phylogenetic Inference in the Genomic Era. Molecular Biology and Evolution. 2020;37(5):1530-4. doi: 10.1093/molbev/msaa015.

103. Yu G, Smith DK, Zhu H, Guan Y, Lam TT-Y. ggtree: an r package for visualization and annotation of phylogenetic trees with their covariates and other associated data. Methods in Ecology and Evolution. 2017;8(1):28-36. doi: https://doi.org/10.1111/2041-210X.12628.

Figure Legends

Fig 1. Deep-sea chronobiology study on the hydrothermal vent shrimp *Shinkaicaris leurokolos*. (A) *S. leurokolos* shrimps (in the green circle) live in the central zone where hydrothermal fluids mix with cold surrounding seawater spontaneously. (B) This work was performed with the *S. leurokolos* colony from the top of the active NBC mound at the Iheya North vent field, Okinawa Trough (126°53.80'E, 27°47.45'N; 982 m depth). (C) Time series of published temperature data covering 351 days recorded at the peripheral area of our sampling site. Lomb-Scargle (LS) periodogram analysis reveals a strong semidiurnal tidal cycle dominated by the M2 tidal constituent, the possible 26.4-hour inertial oscillation is extremely weak. (D) Time series of *in situ* temperature and dissolved oxygen records during 162 seconds when the sensor was placed in the *S. leurokolos* colony showing frequent environmental fluctuations with high variability. (E) Principal components analysis (PCA) plot showing the detrended transcriptomic data from the free-running experiment samples (n = 57). Significance of inter-group differences was examined by the PERMANOVA (*P*-value = 0.376) and ANOSIM (*P*-value = 0.958) analysis both on Bray-Curtis dissimilarities.

Fig 2. The *S. leurokolos* temporal transcriptome was dominated by tidal oscillations under constant conditions. (A) Distribution of the periods of oscillations identified by the eigenvalue/pencil method and the ECHO application. Oscillations with a period range of 10-14 hours and 22-26 hours are regarded as tidal and daily cycling, respectively. (B) Paired *t*-test plot of amplitude for the rhythmic transcripts with both tidal and daily components. (C, D) Venn diagrams detailing the number of rhythmic transcripts (FDR < 0.05) identified by ECHO, RAIN, and eJTK in the tidal range (C) and daily range (D). (E) Raincloud plot of the root mean square (RMS) amplitude for 12-hour tidal transcripts and 24-hour daily transcripts. The stars indicated the level of significance: **** *P*-value < 0.0001.

Fig 3. Free-running tidal transcriptomic patterns of *S. leurokolos*. (A) Density distribution based on amplitude change coefficient (γ) of tidal transcripts detected by ECHO. Oscillation types are categorized as forced ($-0.15 < \gamma < -0.03$; amplified amplitude), harmonic ($-0.03 \leq \gamma \leq 0.03$; steady amplitude), damped ($0.03 < \gamma < 0.15$; reduced amplitude), overexpressed ($\gamma \leq -0.15$), and repressed ($\gamma > 0.15$), and the latter two are considered arrhythmic. (B) Rose chart showing phase distribution comparison of tidal transcripts in cluster 1 and cluster 2. For each oscillation, the phase is divided by period length and then times 360 (degrees) to normalize phases of transcripts with

different period lengths. (C) Heatmap showing highly synchronized gene expression of tidal transcripts (ECHO FDR < 0.05). Each row represents a transcript with three individuals per time point. Transcripts are clustered and ordered by phases, oscillation type, and monotonic trend. Expression of each gene is Z-score normalized. (D) Bubble diagram showing significantly enriched gene ontology (GO) terms related to biological processes of tidal subgroups categorized by three classification schemes (from left to right: cluster, oscillation type, trend). Cross symbols represent a lack of enriched terms in the corresponding subgroup.

Fig 4. Expression profiles of examples of tidal transcripts of interest. The listed tidal genes are potentially involved in various cellular stress response processes, including (A) sulfur metabolism, (B) response to heat or hypoxia, (C) antioxidation and detoxification, and (D) innate immune response. Data points are displayed as mean values ± SEM (n = 3 biological replicates per time point). Normalized expression curves are fitted via the generalized additive model (GAM). Minimum *P*-values of each tidal transcript identified by RAIN, eJTK, and ECHO are presented in the plot.

Fig 5. Expression profiles of core circadian clock genes and opsin genes. (A-G) Temporal expression of *S. leurokolos* homologs of candidate circadian clock genes for (A) PER, (B) TIM, (C) CRY2, (D) CWO, (E) DBT, (F) VRI, (G) PDP1ε. (H-J) Temporal expression of three identified opsin genes, including (H) one long-wavelength-sensitive (LWS) opsin and (I, J) two middle-wavelength-sensitive (MWS) opsins. (K) Opsin expression profile validated by quantitative PCR (qPCR). For RNA-Seq data, data points are displayed as mean values ± SEM (n = 3 biological replicates per time point). For qPCR data, normalized expression curves are fitted via the generalized additive model (GAM). Minimum *P*-values of results from tidal or daily detection of each transcript are presented in the plot. Significant levels of oscillations are indicated with stars: * FDR < 0.05.

Fig 6. A new perspective of biological rhythms in the dark biosphere. Terrestrial and shallow-water organisms largely rely on circadian clocks for anticipating periodic environmental changes such as the day-night transition. Living away from direct sunlight, subterranean mole rats scarcely depend on circadian rhythms for survival, and the endogenous circadian system is understood to be in the process of regression, even though still present. In this work, we found that in addition to the vent mussel *B. azoricus*, the vent shrimp *S. leurokolos* also shows robust free-running gene expression

with a period of approximately 12 hours, likely reflecting the general effects of tidal cycles on deep-sea vent organisms.

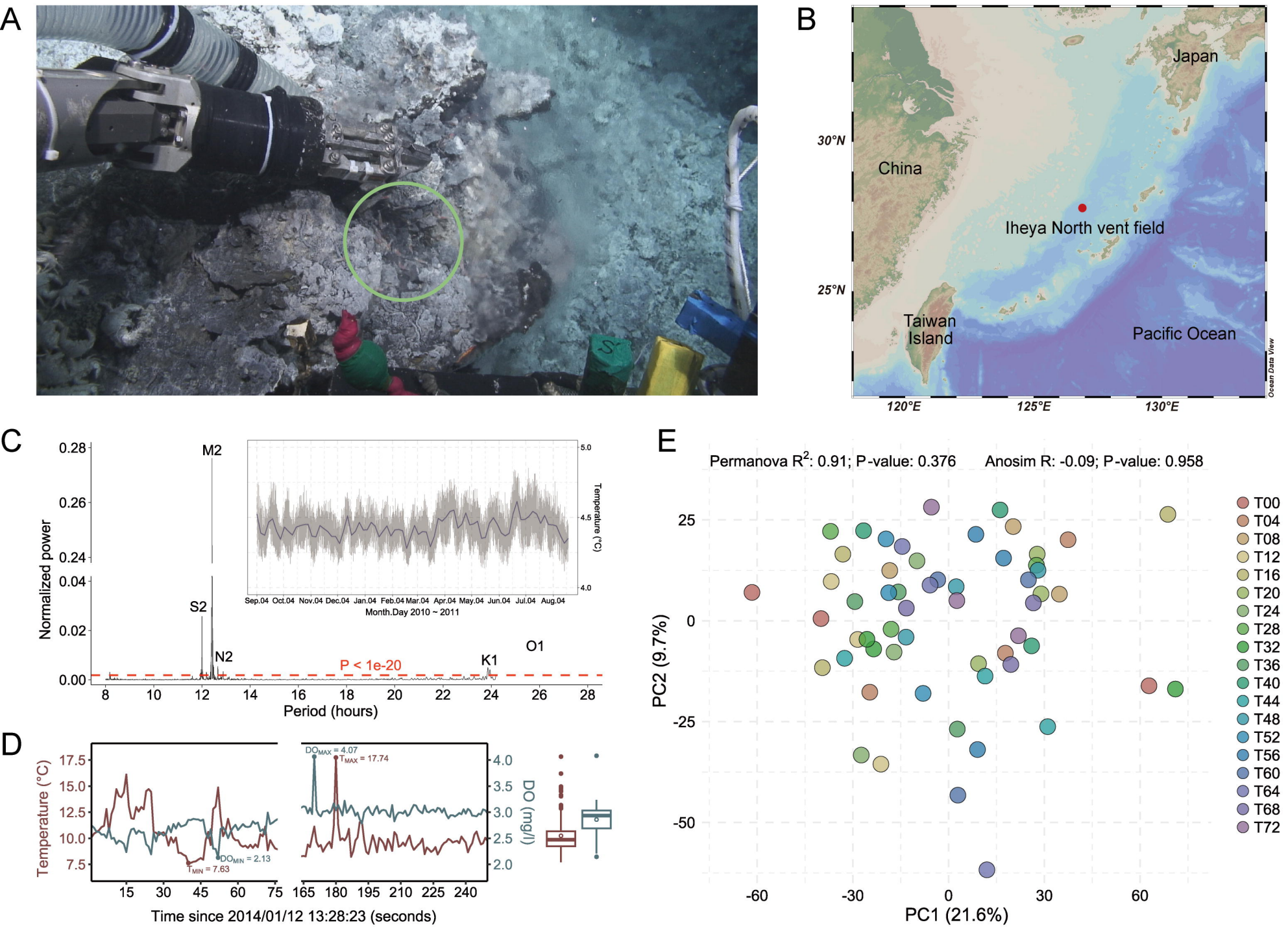
A
B
Japan
30°N
China
Iheya North vent field
25°N
Taiwan Island
Pacific Ocean
Ocean Data View
120°E
125°E
130°E
C
M2
S2
N2
K1
O1
P < 1e-20
Normalized power
Period (hours)
Temperature (°C)
Month.Day 2010 ~ 2011
Sep.04 Oct.04 Nov.04 Dec.04 Jan.04 Feb.04 Mar.04 Apr.04 May.04 Jun.04 Jul.04 Aug.04
D
Temperature (°C)
DO (mg/l)
DO_MAX = 4.07
T_MAX = 17.74
DO_MIN = 2.13
T_MIN = 7.63
Time since 2014/01/12 13:28:23 (seconds)
E
Permanova R2: 0.91; P-value: 0.376
Anosim R: -0.09; P-value: 0.958
PC2 (9.7%)
PC1 (21.6%)
T00
T04
T08
T12
T16
T20
T24
T28
T32
T36
T40
T44
T48
T52
T56
T60
T64
T68
T72

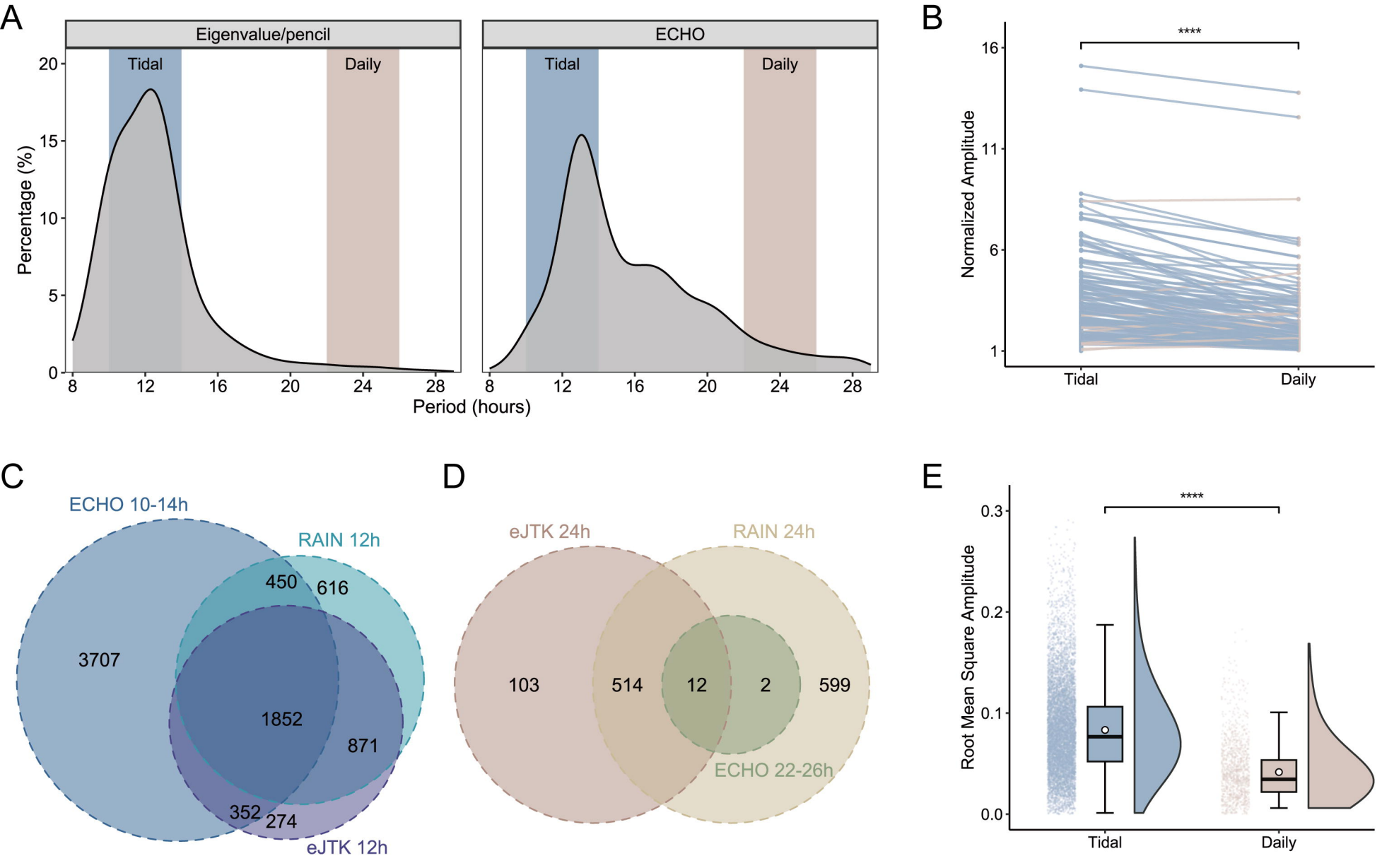
A
Eigenvalue/pencil
ECHO
Tidal
Daily
Percentage (%)
Period (hours)
B
****
Normalized Amplitude
Tidal
Daily
C
ECHO 10-14h
RAIN 12h
eJTK 12h
3707
450
616
1852
871
352
274
D
eJTK 24h
RAIN 24h
ECHO 22-26h
103
514
12
2
599
E
****
Root Mean Square Amplitude
Tidal
Daily

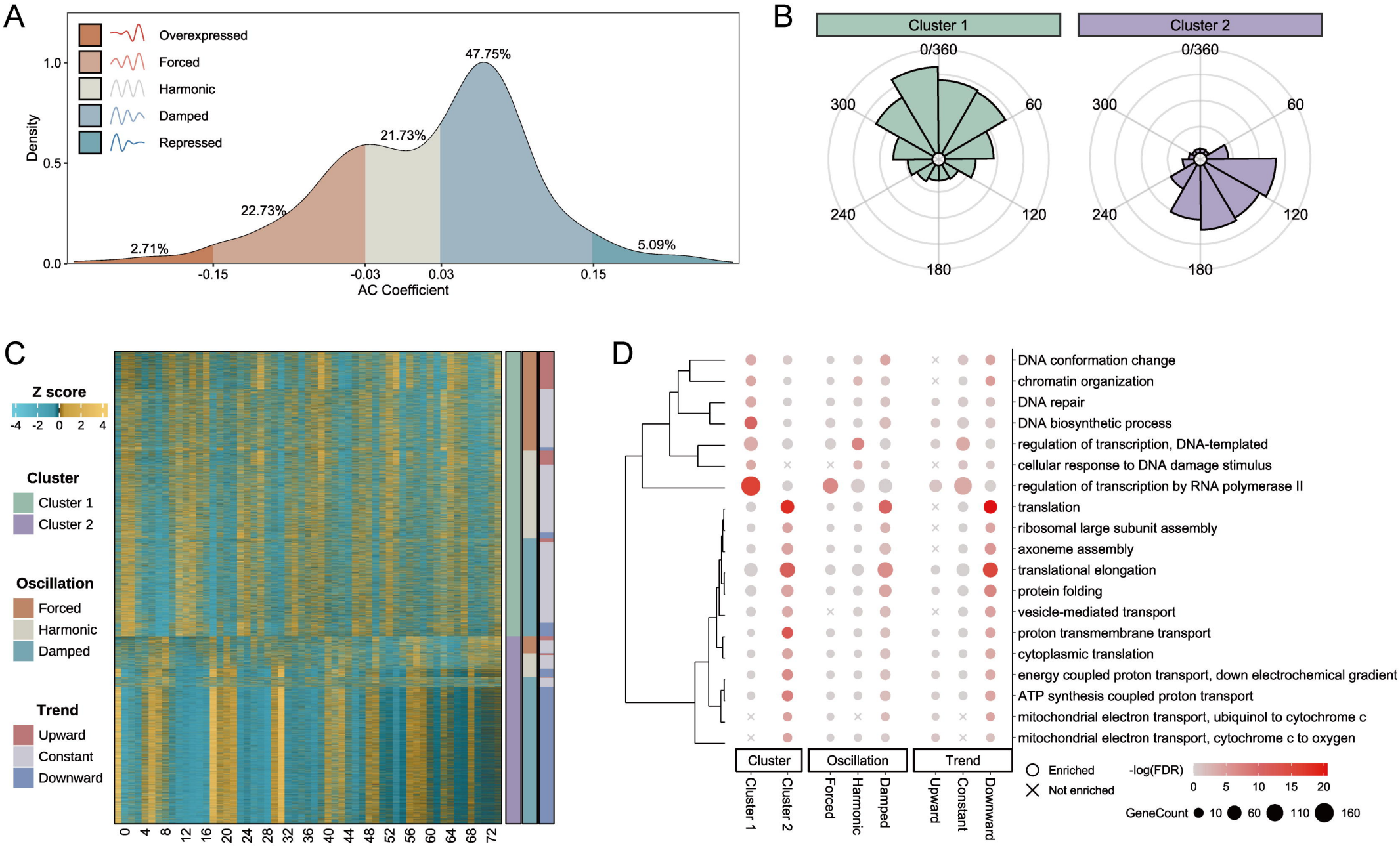
A
Overexpressed
Forced
Harmonic
Damped
Repressed
Density
1.0
0.5
0.0
47.75%
21.73%
22.73%
2.71%
5.09%
-0.15
-0.03
0.03
0.15
AC Coefficient
B
Cluster 1
Cluster 2
0/360
60
120
180
240
300
C
Z score
-4 -2 0 2 4
Cluster
Cluster 1
Cluster 2
Oscillation
Forced
Harmonic
Damped
Trend
Upward
Constant
Downward
0 4 8 12 16 20 24 28 32 36 40 44 48 52 56 60 64 68 72
D
DNA conformation change
chromatin organization
DNA repair
DNA biosynthetic process
regulation of transcription, DNA-templated
cellular response to DNA damage stimulus
regulation of transcription by RNA polymerase II
translation
ribosomal large subunit assembly
axoneme assembly
translational elongation
protein folding
vesicle-mediated transport
proton transmembrane transport
cytoplasmic translation
energy coupled proton transport, down electrochemical gradient
ATP synthesis coupled proton transport
mitochondrial electron transport, ubiquinol to cytochrome c
mitochondrial electron transport, cytochrome c to oxygen
Cluster
Oscillation
Trend
Cluster 1
Cluster 2
Forced
Harmonic
Damped
Upward
Constant
Downward
Enriched
Not enriched
-log(FDR)
0 5 10 15 20
GeneCount
10 60 110 160

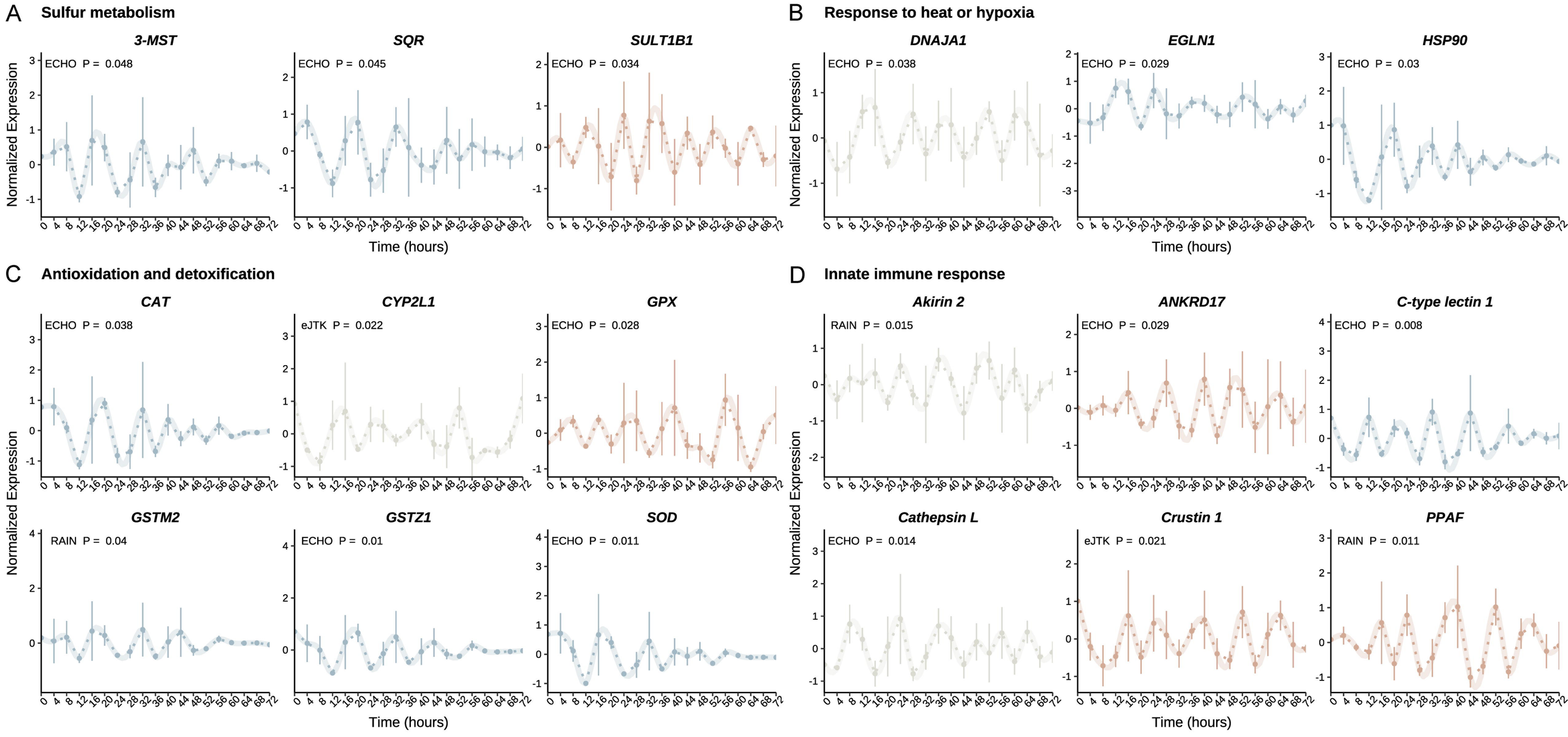
A
Sulfur metabolism
3-MST
ECHO P = 0.048
SQR
ECHO P = 0.045
SULT1B1
ECHO P = 0.034
B
Response to heat or hypoxia
DNAJA1
ECHO P = 0.038
EGLN1
ECHO P = 0.029
HSP90
ECHO P = 0.03
C
Antioxidation and detoxification
CAT
ECHO P = 0.038
CYP2L1
eJTK P = 0.022
GPX
ECHO P = 0.028
GSTM2
RAIN P = 0.04
GSTZ1
ECHO P = 0.01
SOD
ECHO P = 0.011
D
Innate immune response
Akirin 2
RAIN P = 0.015
ANKRD17
ECHO P = 0.029
C-type lectin 1
ECHO P = 0.008
Cathepsin L
ECHO P = 0.014
Crustin 1
eJTK P = 0.021
PPAF
RAIN P = 0.011
Normalized Expression
Time (hours)

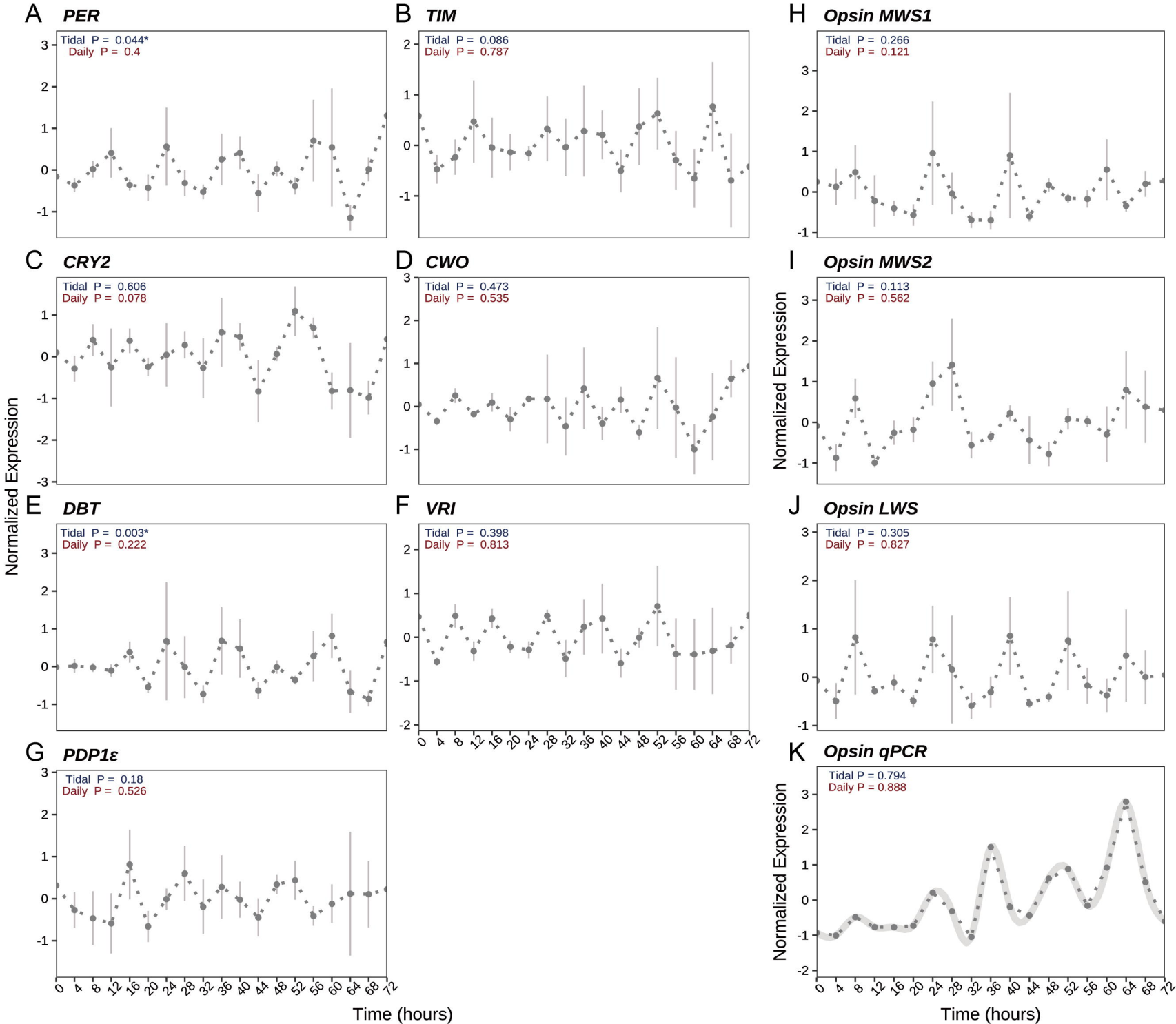
A PER
Tidal P = 0.044*
Daily P = 0.4
B TIM
Tidal P = 0.086
Daily P = 0.787
H Opsin MWS1
Tidal P = 0.266
Daily P = 0.121
C CRY2
Tidal P = 0.606
Daily P = 0.078
D CWO
Tidal P = 0.473
Daily P = 0.535
I Opsin MWS2
Tidal P = 0.113
Daily P = 0.562
E DBT
Tidal P = 0.003*
Daily P = 0.222
F VRI
Tidal P = 0.398
Daily P = 0.813
J Opsin LWS
Tidal P = 0.305
Daily P = 0.827
G PDP1ε
Tidal P = 0.18
Daily P = 0.526
K Opsin qPCR
Tidal P = 0.794
Daily P = 0.888
Normalized Expression
Time (hours)